

OPEN

WAT-on-a-chip integrating human mature white adipocytes for mechanistic research and pharmaceutical applications

Julia Rogal^{1,2}, Carina Binder¹, Elena Kromidas^{1,2}, Julia Roos¹, Christopher Probst¹, Stefan Schneider¹, Katja Schenke-Layland^{2,3,4} & Peter Loskill^{1,2*}

Obesity and its numerous adverse health consequences have taken on global, pandemic proportions. White adipose tissue (WAT) – a key contributor in many metabolic diseases – contributes about one fourth of a healthy human's body mass. Despite its significance, many WAT-related pathophysiological mechanisms in humans are still not understood, largely due to the reliance on non-human animal models. In recent years, Organ-on-a-chip (OoC) platforms have developed into promising alternatives for animal models; these systems integrate engineered human tissues into physiological microenvironment supplied by a vasculature-like microfluidic perfusion. Here, we report the development of a novel OoC that integrates functional mature human white adipocytes. The WAT-on-a-chip is a multilayer device that features tissue chambers tailored specifically for the maintenance of 3D tissues based on human primary adipocytes, with supporting nourishment provided through perfused media channels. The platform's capability to maintain long-term viability and functionality of white adipocytes was confirmed by real-time monitoring of fatty acid uptake, by quantification of metabolite release into the effluent media as well as by an intact responsiveness to a therapeutic compound. The novel system provides a promising tool for wide-ranging applications in mechanistic research of WAT-related biology, in studying of pathophysiological mechanisms in obesity and diabetes, and in R&D of pharmaceutical industry.

The global obesity pandemic poses one of today's biggest challenges to public health. Each year, 2.8 million people die from causes related to overweight or obesity¹. Since the 1970s, the worldwide prevalence of obesity has nearly tripled, also leading to an upsurge in associated comorbidities such as type 2 diabetes (Fig. 1a)². Future projections reveal the gravity of this public health crisis: the prevalence rates of childhood obesity are increasing at an alarming pace³, and by 2030, more than 50% of U.S. adults are predicted to be obese⁴. White adipose tissue (WAT) is the principal organ in obesity. In healthy human adults, WAT comprises approximately 20–25% of the total body mass, thus constituting the second largest organ, after the skin. In obese individuals, WAT's contribution to the total body mass may become as high as 50% (Fig. 1b)⁵.

WAT is tightly involved in the two most important functions of an organism – energy homeostasis and reproduction⁶. In energy homeostasis, not only does WAT act as the main storage site of excess dietary energy (Fig. 1c), it also performs crucial endocrine and metabolic functions (Fig. 1d)^{7,8}. WAT can sense the body's energy status, and respond appropriately, either by storing fuel, in the form of triacylglycerides, or by releasing it as glycerol and fatty acids, for ultimate delivery to organs in need. While this classically described role of WAT already entailed extensive crosstalk between WAT and other organs, its inter-organ communications extend beyond simple feedback loops activated by fed- or fasted states. Endocrine functions of white adipocytes, and other WAT-resident cells in the stromal vascular fraction, are performed by the release of a variety of adipokines (adipose-associated

¹Fraunhofer Institute for Interfacial Engineering and Biotechnology IGB, Nobelstrasse 12, 70569, Stuttgart, Germany. ²Department of Women's Health, Research Institute for Women's Health, Eberhard Karls University, Calwerstrasse 7, 72076, Tübingen, Germany. ³NMI Natural and Medical Sciences Institute at the University of Tübingen, Markwiesenstr. 55, 72770, Reutlingen, Germany. ⁴Department of Medicine/Cardiology, Cardiovascular Research Laboratories, David Geffen School of Medicine at UCLA, 675 Charles E. Young Drive South, MRL 3645, Los Angeles, CA, USA. *email: peter.loskill@igb.fraunhofer.de

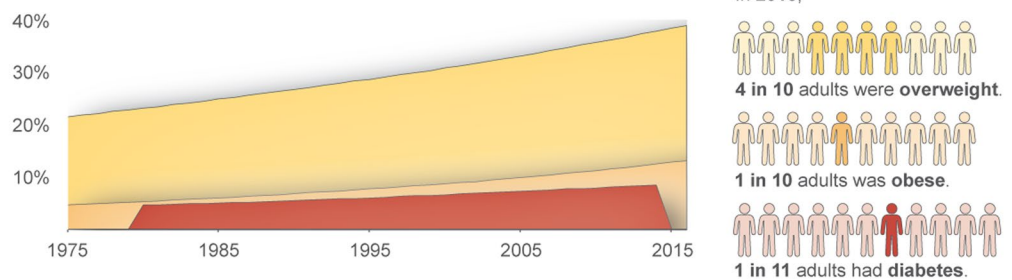
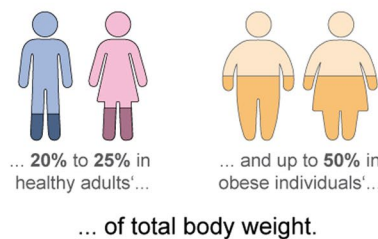
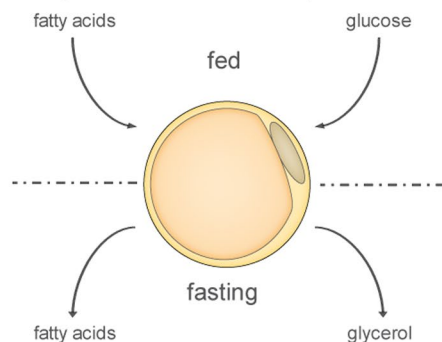
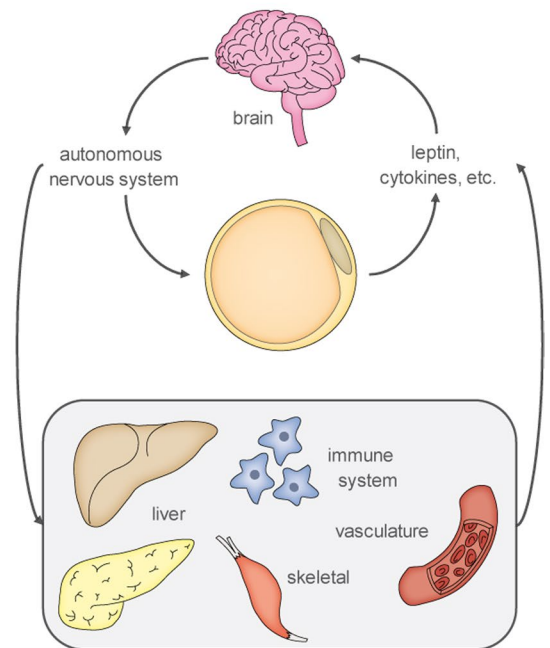
a. Prevalence of overweight, obesity and diabetes.**b. White adipose tissue comprises...****c. Storage function of white adipose tissue.****d. Endocrine function of white adipose tissue.**

Figure 1. Relevance of research on WAT. **(a)** The worldwide prevalence of obesity has nearly tripled since 1975; in 2016, almost 40% of adults aged 18 and over could be classified as overweight, 13% of them were even obese. This developments has coincided with a rising prevalence of diabetes, which in 2016 affected approximately 9% of adults worldwide. T2DM – the most prevalent form of diabetes – often develops during chronic positive energy balance, e.g., by a combination of excessive energy intake and physical inactivity^{1,2}. **(b)** WAT's contribution to body mass is 20–25% in healthy individuals, and up to 50% in the obese⁵. **(c)** Traditional view of WAT as an organ primarily for energy storage. **(d)** Additional, modern-day concepts of WAT functionality, including extensive endocrine functions.

cytokines) which affect the functioning of the brain, liver, pancreas and immune system⁹. Besides managing nutritional homeostasis, WAT contributes to the regulation of the hypothalamic-pituitary-gonadal axis by secreting and metabolizing sex steroids⁷. Especially adipose tissue intracrinology, i.e., the modulation of sex steroid levels by significant numbers of locally expressed enzymes that activate, convert, or inactivate circulating steroid hormones, plays important roles in human reproductive function^{7,10,11}. Given its prominent endocrine functions and extensive cross-talk with other organs, it comes as little surprise that abnormal amounts, or altered functioning of WAT may result in wide-ranging disorders, including hepatic and cardiovascular diseases^{12,13}, diabetes and cancer^{14–16}.

In line with its important roles in metabolism, inflammation and cancer, WAT has emerged as a drug target with major therapeutic potential for a variety of diseases^{17–19}. Additionally, storage metabolism by WAT can have a major impact on the efficacy of drug therapies, such as those for cardiovascular diseases and cancer^{20,21}. For instance, adipocytes may metabolize and inactivate the chemotherapeutic Daunorubicin²¹, which strongly affects the efficacy of this anticancer therapeutic. Furthermore, the capacity of WAT to sequester hydrophobic compounds, gives the tissue a prominent role in absorption, distribution, metabolism, and excretion (ADME) processes.

Even though WAT plays such a significant role in many diseases, surprisingly little is known about pathophysiological processes of WAT, especially when considering the ever-increasing prevalence of obesity and its co-morbidities. An important reason for this lacking insight is that mechanistic studies in humans often involve

unacceptable health risks. Hence, most research depends on clinical observation, genome-wide association studies (GWAS) as well as animal studies²². Although animal models have led to many insights in obesity and diabetes, they often are lacking in predictive validity for human body functioning, first because of important species differences in nutrition and metabolism, and second because the distinct, unique physiological and pathophysiological roles of WAT in humans²³. Alternatively, conventional, cell culture-based *in vitro* models have been widely utilized and are significantly less controversial ethically. Typically, researchers have used a variety of cell sources, ranging from (immortalized) murine, to primary human (pre-)adipocytes, each featuring distinct advantages and limitations²⁴. *In vitro* differentiation of adipogenic progenitor cells, i.e., either pre-adipocytes or multipotent stem cell lines, or (induced) pluripotent stem cells, is often the method of choice due to the availability of donor-specific information, and the capacity of these cells to undergo expansion and cryopreservation while retaining their characteristic fat depot. Yet, the *in vitro* use of differentiated adipocytes has two major drawbacks: unlike their *in situ* matured congeners, (i) their lipid contents never reach a state of unilocularity, but remain distributed among multiple small lipid vacuoles, and (ii) their gene expression and secretome differs significantly in the relative proportions of adipose-associated hormones^{25–27}. Both phenomena reflect a pre-mature state of the *in vitro* differentiated adipocytes, which strongly suggests that mature human adipocytes provide the best recapitulation of a mature human adipocyte physiology. Yet, the *ex vivo* culture of primary human adipocytes is extremely challenging, due to issues with the cells' buoyancy, fragility and de-differentiation, which so far have hindered development of robust protocols for long-term culturing. Similarly, studies using whole WAT explants are restricted to short culture durations. Additionally, inter-individual variability complicates the interpretation of study results based on samples from different donors²⁸.

Overall, it is of utmost importance to develop microscale platforms that provide microphysiological environments for the long-term culture of white adipocytes in structures that may recapitulate *in vivo* physiology, and functionality based on a minimal amount of cells. By combining modern techniques in microfabrication, biomaterials and tissue engineering, organ-on-a-chip technology has enabled the construction of promising platforms for mechanistic and pharmaceutical studies, that have great potential for disease modeling as well as the optimization of personalized medical treatments of obesity and diabetes^{29–32}. The integration of tissues with *in vivo*-like structure and functionality in perfused microenvironments is of particular interest when studying endocrine tissues and multi-factorial diseases, due to the possibility to combine individual chips into multi-organ systems^{33,34}. However, although organ-on-a-chip research has burgeoned in recent years, and numerous platforms have been developed for many organs and tissues, WAT appears to have been largely overlooked, and only a few relevant efforts have been undertaken²⁵. Several research groups injected pre-adipocytes from murine^{35,36} or human^{37–39} sources into microfluidic chambers, and were able to subsequently induce adipogenesis. Others directly introduced primary adipocytes from mice into mesoscopic, perfused reservoirs⁴⁰. In a recently introduced elegant approach, Harms *et al.* cultured mature human white adipocytes in multiwell plates underneath membranes in a transwell format⁴¹. All of these innovative approaches, however, did not enable the generation of human white adipose tissue-like structures with *in vivo*-like physiology.

Here, we present the first OoC platform that integrates human primary mature adipocytes into a perfused microfluidic chip. The human WAT-on-a-chip consists of multiple, tissue-specific chambers that are fluidically connected to a vasculature-like microchannel, while being shielded from the shear forces of the perfusion fluid. Using specifically tailored isolation and injection protocols, 3D microtissues based on freshly isolated adipocytes are generated inside a series of individual chambers. Thus, a large number of independent replicate cell cultures from individual donors can be produced and kept viable – as well as functional – for over one month. By analyzing media effluents and taking advantage of the optical accessibility of the tissue chambers, the patency of cells as well as key cell-physiological aspects, e.g., fatty acid metabolism and drug responsiveness, could be monitored successfully.

Materials and Methods

Fabrication and characterization of microfluidic platforms. *Chip fabrication by soft lithography and replica molding.* The microfluidic platform is a custom-designed three-layered hybrid device featuring two micro-patterned polydimethylsiloxane (PDMS; Sylgard 184, Dow Corning, USA) layers, which are separated by an isoporous semipermeable membrane. The media channel and tissue chamber microstructures in the PDMS slabs were generated using two differently patterned master wafers that served as positive molding templates. The intricately structured masters were fabricated by commonly used photolithographic processes described previously³⁶. The chips' PDMS structures were created using two different molding techniques: standard molding to obtain thicker slabs with closed structures, and exclusion molding to obtain thin layers with open structures (cf. "Replica molding of PDMS parts" in the supplements section). To prepare the semipermeable membranes, commercially available polyethylene terephthalate (PET) membranes ($r_p = 3 \mu\text{m}$; $\rho_p = 8 \times 10^5$ pores per cm^2 ; TRAKETCH® PET 3.0 p S210 \times 300, SABEU GmbH & Co. KG, Northeim, Germany) were functionalized by a plasma-enhanced, chemical vapor deposition (PECVD) process (cf. "Membrane functionalization" in the supplements section). In a final step, chips were assembled in three subsequent O_2 -plasma activation (15 s, 50 W; Diener Zepto, Diener electronic GmbH + Co. KG, Ebhausen, Germany) and bonding steps, followed by an overnight exposure to 60 °C for bonding enhancement (cf. "Chip assembly" in the supplements section).

Chip preparation for experiments. On the day before cell injection, chips were O_2 -plasma sterilized (60 s, 50 W) and subsequently filled with Dulbecco's phosphate-buffered saline without MgCl_2 and CaCl_2 (PBS^- ; Sigma-Aldrich Chemie GmbH, Steinheim, Germany), under sterile conditions. Then, the PBS^- filled chips were kept overnight at 4 °C in PBS^- to allow evacuation of residual air from the channel systems.

Numerical modeling. To model fluid flow and transport of a diluted species, COMSOL Multiphysics (COMSOL, Stockholm, Sweden) software was used. The process was based on a numerical model which was previously published for our previous murine WAT-on-a-chip³⁶. Briefly, the incompressible stationary free fluid flow was modeled by the Navier-Stokes equation with the properties of water (dynamic viscosity $\mu = 1 \times 10^{-3}$ m²/s, density $\rho = 1000$ kg/m³) at a flow of 20 μ l/h. Fluid flow from the media channel through the isoporous membrane into the tissue chamber was modeled using Darcy's law (porosity = 0.056, hydraulic permeability $\kappa = 1.45 \times 10^{-14}$ m²). The transport of diluted species was described by the time-dependent convection-diffusion with a diffusion coefficient 1×10^{-9} m²/s and an initial concentration of 1 mol/m³.

Diffusive transport. To visualize diffusion of compounds from the media microchannels over the isoporous membrane into the tissue chamber inside the microfluidic platform, we monitored the perfusion of a 0.5 mg/ml fluorescein isothiocyanate–dextran (FITC–dextran; 150 kDa, 46946, Sigma-Aldrich Chemie GmbH) solution in PBS⁻ in the system. Prior to the diffusion experiment, the tissue chambers were filled with the collagen hydrogel matrix commonly used to encapsulate the adipocytes (cf. “Injection of human mature adipocytes into the microfluidic platform”). The flow rate was set to 40 μ l/h and the fluorescence intensity was measured every 6.2 s for three positions in the chip – the media channel, the top of the underlying tissue chamber, as well as the bottom of the same tissue chamber.

Isolation and culture of primary human adipocytes. *Human tissue samples.* Human adiposetissue biopsies were obtained from plastic surgeries performed by Dr. Ulrich E. Ziegler (Klinik Charlottenhaus, Stuttgart, Germany), approved by the local medical ethics committee: Patients gave an informed consent according to the permission of the “Landesärztekammer Baden-Württemberg” (IRB#: F-2012-078; for normal skin from elective surgeries). All procedures were carried out in accordance with the rules for medical research of human subjects, as defined in the Declaration of Helsinki. All primary mature adipocytes were isolated from biopsies that were taken from female, pre-obese donors (BMI 25.0 - 29.9, as per the WHO classification), aged 45 to 55.

Isolation of primary human adipocytes. Primary mature adipocytes were isolated from subcutaneous adipose tissue samples. The isolation protocol was performed as previously described^{42,43}, with slight modifications. In brief, the subcutaneous adipose tissue was rinsed twice with Dulbecco's phosphate buffered saline with MgCl₂ and CaCl₂ (PBS⁺; Sigma-Aldrich Chemie GmbH), and visible blood vessels, as well as connective-tissue structures, were thoroughly removed. The remaining adipose tissue was cut into fine pieces of approximately 1 cm³, and digested with a collagenase solution [(0.13 U/ml collagenase type NB4 (Serva Electrophoresis GmbH, Heidelberg, Germany) in Dulbecco's Modified Eagle Medium (DMEM/Ham's-F12; Thermo Fisher Scientific, Waltham, USA), with 1% bovine serum albumin (BSA; Sigma-Aldrich Chemie GmbH)] for 60 min at 37 °C on a rocking shaker (50 cycles/min; Polymax 1040, Heidolph Instruments GmbH & CO. KG, Schwabach, Germany). Next, the digested tissue was passed through cell strainers (mesh size: 500 μ m), and subsequently washed three times with DMEM/Ham's-F12. For each washing step, adipocytes and medium were mixed, and left to rest for 10 min to allow separation of the buoyant adipocytes and the medium; this was followed by aspiration of the liquid media from underneath the packed layer of adipocytes.

Injection of human mature adipocytes into the microfluidic platform. Immediately after the isolation of white adipocytes from tissue samples, the adipocytes were prepared for injection into the microfluidic platforms. Sixty μ l of densely packed adipocytes were mixed with 24 μ l of a dispersion of 10 mg/ml collagen type 1 (from rat tail, provided by Fraunhofer IGB), 6 μ l neutralization buffer [DMEM/Ham's F-12 (10 \times); Biochrom GmbH, Berlin, Germany), and 50 mM NaOH in Aqua dest (1:1) with 0.2 M NaHCO₃ and 0.225 M HEPES (Carl Roth GmbH + Co. KG, Karlsruhe, Germany)] and immediately injected into the chip's tissue-chamber system by manual pressure. Each system of connected tissue chambers was loaded individually at a steady pace, to ensure that the collagen hydrogel reached the tissue chambers before the onset of gelation.

On-chip culture of adipose tissue. During on-chip culturing, the WAT-chips were maintained in a humidified incubator at 37 °C and a 5% CO₂ atmosphere. The adipocytes were supplied with a 20–40 μ l/h flow of Subcutaneous Adipocyte Maintenance Medium (AM-1; BioCat GmbH, Heidelberg, Germany) maintained by positive pressure from an automated syringe pump (LA-190, Landgraf Laborsysteme HLL GmbH, Langenhagen, Germany). Under sterile conditions, media reservoirs were re-filled with fresh media every other day, and the media effluents were collected from the media-systems' outlets once every 1–2 days (depending on the experiment), and stored at –80 °C for subsequent analysis of metabolites.

Structural and functional characterization of on-chip adipose tissues. *Fluorescent double staining of intracellular lipid vacuoles and nuclei.* To visualize the structure of on-chip adipose tissues, intracellular lipid vacuoles and nuclei were stained using the neutral lipid stain BODIPYTM 493/503 (4,4-Difluoro-1,3,5,7,8-Pentamethyl-4-Bora-3a,4a-Diaza-s-Indacene; D3922, Thermo Fisher Scientific) and 4',6-Diamidin-2-phenylindol (DAPI; D8417, Sigma-Aldrich Chemie GmbH). All fixation- and staining solutions were flushed through the chip at a rate of 80 μ l/h by a syringe pump. The in-chip adipocytes were fixed overnight with 4% phosphate-buffered formaldehyde solution (Roti[®]-Histofix 4%, P087, Carl Roth GmbH + Co. KG). Next, permeabilization was achieved by flushing the chip for 3 h with PBST [PBS⁺ with 0.1% Tween-20 (P7949, Sigma-Aldrich Chemie GmbH)]. Then, the fluorescence staining solution – PBST with 1 μ g/ml BODIPYTM 493/503 and 1 μ g/ml DAPI – was pumped through the system for 2 h, and finally washed out with PBS⁺ for at least 30 min to remove residual staining solution. To stain explants, chunks of approximately 100 mm³ were cut off from the biopsy, washed with PBS + twice and fixed for 1 h with 4% phosphate-buffered formaldehyde solution.

Afterwards, the fixed explants were washed with PBS⁺, permeabilized and stained as described above (1 h of incubation time for each step). Finally, the explants were washed three times in PBS⁺ to remove residual staining solution and stored in PBS⁺ until imaging.

Imaging of the stained adipocytes was performed and processed by a laser scanning microscope (Zeiss LSM 710, Carl Zeiss, Oberkochen, Germany) with specialized software (ZEN 2012 SP1 (black edition), Release Version 8.1)).

Live/dead staining of integrated white adipose tissue. To assess the viability of the adipocytes on-chip, a live/dead-assay based on fluorescein diacetate (FDA; F1303, Thermo Fisher Scientific) and propidium iodide (PI; P3566, Thermo Fisher Scientific) was performed. Prior to staining, the culture medium was removed from the chip by flushing the media channels with PBS, using gravitational flow. The staining solution containing FDA (final concentration 27 µg/ml) and PI (final concentration 135 µg/ml) diluted in PBS, was flushed into the media channel by gravitational flow, and incubated for 25 min in a humidified incubator at 37 °C and 5% CO₂. The staining solution was then removed by flushing PBS through the media channels using gravitational flow. Right after that, imaging was performed by an inverted fluorescence microscope (Leica DMi8, LEICA Microsystems GmbH, Wetzlar, Germany).

Monitoring and analysis of fatty acid uptake and release. For online monitoring of fatty acid uptake by the adipocytes, 4 µM of the fluorescently-labeled fatty acid analog, BODIPYTM 500/510 C1, C12 (4,4-Difluoro-5-Methyl-4-Bora-3a,4a-Diaza-s-Indacene-3-Dodecanoic Acid; D3823, Thermo Fisher Scientific), was added to the culture medium for a duration of 60 min and pumped through the media systems at 80 µl/h via positive pressure provided by a syringe pump. Next, the culture medium was switched to AM-1 only, to visualize the release of the fluorescent fatty acid analog. During the experiment, the chips were placed under complete darkness in an incubator chamber that was fitted to the microscope stage, and set to 37 °C. Imaging was performed using the inverted Leica DMi8 fluorescence microscope. During the 120 min running time of the experiment, images of both bright-field (BF) and FITC-channels were captured every two minutes from each tissue chamber on the chip. As a reference, each position was imaged at time point 0 min (t₀).

To quantify the patterns of fluorescence intensity during the uptake and release of the fluorescent fatty acid analog, the mean gray value of the fluorescence of the individual tissue chambers and the fluorescence of the background were measured for each time point using ImageJ 1.50i software (National Institute of Health, Bethesda, USA). After subtracting the background levels from the fluorescence intensities measured in the chambers, the offset was calculated by setting the intensity measured at t₀ to a fluorescence intensity of 0 A.U. Then, the intensities for each chamber were expressed as a percentage of the highest recorded intensity from that chamber during the experiment. Note: Normalization on the chamber-level was considered to be necessary, because the amount of injected adipocytes varied between the chambers with the used WAT-chip design.

Responsiveness to β-adrenoreceptor agonistic drugs. To assess the effect of β-adrenergic agonist drugs on fatty acid metabolism, AM-1 medium was supplemented with 10 µM isoproterenol hydrochloride (I6504, Sigma-Aldrich Chemie GmbH). Fluorescence intensity was measured for 60 min with, and then for 60 min without addition of 4 µM BODIPYTM 500/510 C1, C12 to the conditioned medium at 37 °C with an inverted fluorescence microscope (LEICA DMi8, LEICA Microsystems GmbH) to assess the dynamics of fatty acid uptake and release. Measurement and analysis of fluorescence was performed as described above.

Non-invasive analysis of cytotoxicity from media effluents. The release of lactate dehydrogenase (LDH) was quantified from the media effluents to non-invasively assess the adipocytes' on-chip viability. The medium effluents were collected for a sampling time of 24 h on different days of on-chip culture. For analysis of the medium effluents, we used the CytoTox 96[®] Non-Radioactive Cytotoxicity Assay (G1780; Promega GmbH, Walldorf, Germany) and followed the manufacturer's instructions for performing the assay in a 384-well plate format. This assay allows for colorimetric the detection of necrotic and late-stage apoptotic cells. For a Target Cell Maximum LDH Release Control, adipocytes were injected into two chips as described above. After injection, the adipocytes were perfused with lysis buffer for 2 h until all adipocytes were lysed. The mean of the acquired absorbance was assumed to be the maximum LDH release possible for the given experimental setup including chip design and adipocyte donor. All other acquired LDH data were normalized to this value.

Analysis of adipose-associated metabolites. The non-esterified fatty acid (NEFA) contents of medium effluents were determined by enzymatic analysis, using the ACS-ACOD-MEHA method (NEFA-HR(2) Assay, FUJIFILM Wako Chemicals Europe GmbH, Neuss, Germany). Effluents were thawed and centrifuged at 10,000 × g for 10 min. Then, 25 µl of sample [i.e. the effluents' supernatant, or AM-1 as blank, or oleic acid for a standard curve (270-77000, FUJIFILM Wako Chemicals Europe GmbH)] were supplemented with 100 µl of the R1 solution (434-91795, FUJIFILM Wako Chemicals Europe GmbH) and 50 µl of the R2 solution (436-91995, Wako Chemicals GmbH), incubating 10 min at 37 °C after each addition. NEFA concentrations were determined by measuring absorbance at 550 nm (Infinite[®] 200 PRO, Tecan Trading AG, Switzerland). To assess the influence of albumin on NEFA release, 0.2% human serum albumin (HSA; A1653, Sigma-Aldrich Chemie GmbH) was added to the culture medium for 24 h. To ensure that increases in the measured NEFA concentrations could not be attributed to the presence of HSA during assay performance, we performed NEFA-measurements on the oleic acid standard with and without HSA. No differences were observed in the detected NEFA-concentration between the two conditions (Fig. S4).

As another readout for lipolysis, glycerol concentrations were determined using a colorimetric assay. Media effluents were thawed and centrifuged at 10,000 × g for 10 min. Then, 40 µl of sample [i.e. the effluents' supernatants, or AM-1 as blank, or Glycerol Standard Solution for a standard curve (G7793, Sigma-Aldrich Chemie

GmbH)] were supplemented with 60 μl of the Free Glycerol Reagent (F6428, Sigma-Aldrich Chemie GmbH). After a 5-min incubation at 37 °C, absorbance at 540 nm was recorded.

Statistical analysis. All graphs show raw data means \pm standard deviation (unless otherwise indicated). We annotated or sample size n as follows:

- For analyses pertaining to data at tissue chamber level (e.g. from fatty acid transport assays), n denotes the number of tested tissue chambers.
- For analyses pertaining on tissue system level only, i.e., the collectivity of eight chambers connected via one media channel, (e.g. metabolite measurements), n denotes the number of tested tissue systems.

For statistical analysis of differences, we performed independent two-sample t -tests using OriginPro 2018 software (OriginLab, Northhampton, MA, USA). Unless otherwise indicated, a p -value threshold for significance of 0.05 was used.

Results and Discussion

Concept and characterization of the microfluidic platform. In order to generate a microphysiological environment capable of generating a human WAT-model, and maintaining tissue viability and functionality during long-term culture, we developed a specifically tailored microfluidic platform featuring a footprint comparable to the size of a stamp ($2 \times 2 \text{ cm}$). The essential features of the platform, depicted in Fig. 2a, are 3D-tissue chambers and perfusable microchannels that are separated by an isoporous membrane. Each chip platform houses two identical, independent systems each featuring eight individual tissue chambers. All tissue chambers are located at the end of individual branches of a main channel, which can be accessed via a common inlet for cell injection. The tissue chambers are specifically designed to accommodate adipose tissue, particularly its large-sized, fragile and buoyant adipocytes: they are cylindrical structures with a diameter of 720 μm and a height of 200 μm . The tissue-chamber microstructures are encased by transparent glass (cover slip or microscope slide) at the bottom, enabling easy visual inspection of the tissues with most current types of microscope, and by an isoporous membrane on the top side. The membrane was specifically functionalized (Supplement S2) to ensure a tight sealing of chip components, and to provide a porous barrier to the adjacent media microchannels. The channels can be connected to external devices (e.g. syringe- or peristaltic pumps), to achieve a vasculature-like perfusion with media. This allows for a precisely controllable convective transport of nutrients, metabolites, and other dissolved molecules towards, as well as away from, the tissue chambers, mimicking the *in vivo* circulation of blood. It also opens up the possibility to administer compounds with high temporal resolution. The membrane further ensures that convective transport is restricted to the media channels, thereby shielding the tissue chambers from non-physiological shear forces (Fig. 2b). Through the micropores, dissolved molecules may diffuse quickly in and out of the tissue chambers, as confirmed by computational modeling and by dynamic tracking of a fluorescent dye in different channel- and chamber locations (Fig. 2b). In sum, the membrane constitutes an endothelial-like barrier that separates perfused media from the chip-embedded tissues. Although this artificial barrier admittedly does not recapitulate active transport processes occurring *in vivo*, it does provide a potential scaffold for the inclusion of endothelial cells in future generations of the platform.

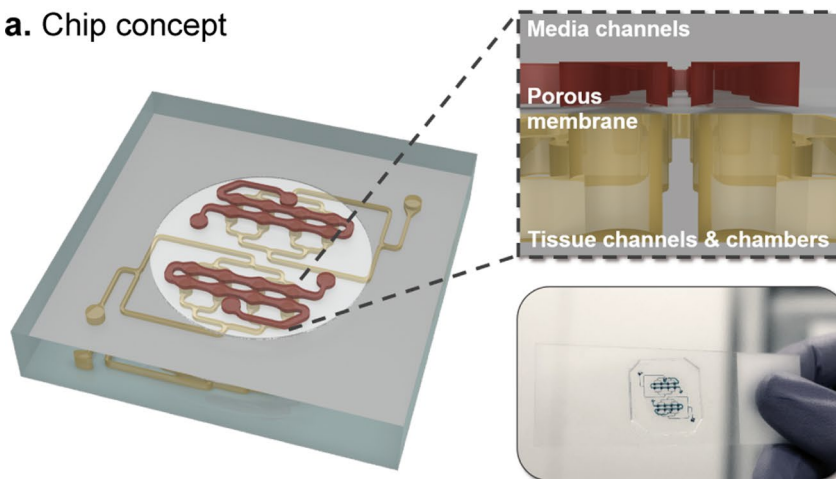
Generation and functional validation of human white adipose tissue on-chip. Two major difficulties of mature adipocytes – their buoyancy and fragility – have traditionally hampered the *in vitro* culture of WAT. We developed specifically optimized cell-isolation and -injection protocols to enable the integration of freshly isolated, mature primary adipocytes from humans into the tissue chambers of our microphysiological platform. By suspending the isolated cells into a collagen hydrogel before injection, their viability and integrity could be preserved. The use of the hydrogel ensures both the protection and the 3D arrangement of the fragile cells during the formation of the microtissue. Moreover, the hydrogel and the location of the cell-injection inlets on the bottom of the tissue chambers (Figs. 2a and 3) help to overcome the issue of adipocyte buoyancy. Successful cell loading generates 8 independent, parallel 3D WAT-like microtissues per system (and 16 per platform).

Due to the microscale footprints of chambers and platform, only a small number of cells are required per chamber. This is of particular importance, as the tissues are based on primary, non-proliferating cells, and multiple chips (independent replicates) can be loaded with cells from a single biopsy, enabling testing under multiple experimental and control conditions of microtissues from the same donor. This is of crucial advantage when dealing with inter-donor variability, while it also enables patient-specific experiments.

Structural analysis of adipocytes on-chip. To investigate the structural arrangement of the generated adipose tissue, we established a staining protocol that enabled the on-chip visualization of intracellular lipid vacuoles using a neutral lipid stain. After six days of on-chip culturing, confocal imaging confirmed the formation of dense, 3D tissues composed of large unilocular adipocytes (Fig. 3a). The observable, mature phenotype of adipocytes suggests that the tissue-generation and -culture methods were capable of creating and maintaining physiological microenvironments and conditions. Inappropriate culture conditions have been frequently reported to induce cell dedifferentiation^{43,44} which would lead to highly proliferative dedifferentiated fat cells (DFAT) with multilineage character⁴⁵. One of the first hallmarks of dedifferentiation is the re-organization of lipids into multiple lipid droplets (i.e., a multilocular phenotype) and an increased rate of lipolysis⁴⁴.

Moreover, we analyzed the microfluidic platform for a potential selectivity in terms of adipocyte structure by comparing the size of the lipid vacuoles of adipocytes on-chip to that of the respective donor-specific explants (Fig. 3b). Due to the unilocularity of mature adipocytes, determining lipid droplet size is an indirect measure for the adipocytes' size. The quantitative analysis revealed that both average size as well as the distribution of

a. Chip concept



b. Separation of transport processes

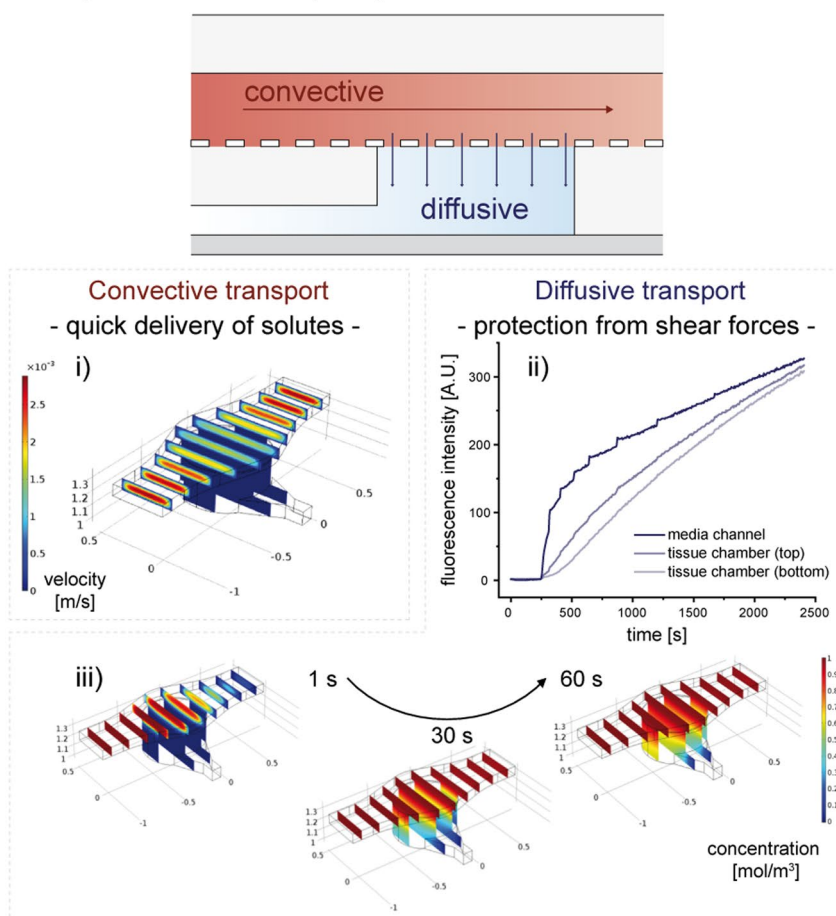


Figure 2. Concept of the microphysiological platform and microfluidic perfusion. **(a)** Schematic of the chip platform featuring two independent systems with eight tissue chambers each. As shown in the cross-sectional zoom-in, tissue chambers, which feature tissue channel inlets at the bottom, are located right below the perfusable media channels, and separated from them by a microporous membrane. **(b)** During flow, the chip's circuitry imposes a separation of the two transport processes, convection and diffusion. Convective flow is confined to the vasculature-like media channels, as confirmed by computational modeling (i). The tissue chambers are supplied by a diffusive transport as confirmed by observable diffusion of a fluorescent dye from the media channel into a hydrogel-filled tissue chamber (ii), as well as by computational modeling (iii).

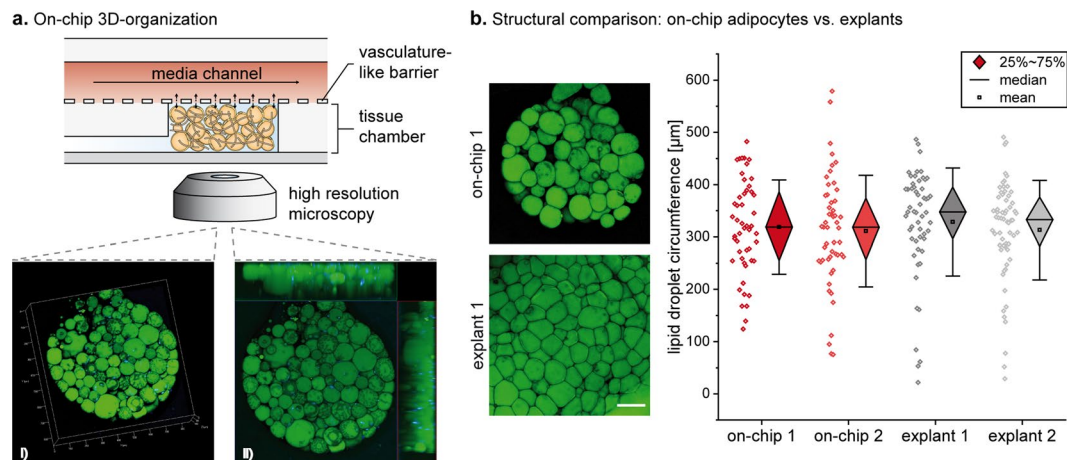


Figure 3. Structural characterization of human WAT-on-a-chip. **(a)** On day 6 of on-chip culture, intracellular lipid vacuoles (green; neutral lipid stain BODIPY™ 493/503) and nuclei (blue; DAPI) were visualized by confocal imaging. As shown by a 3D-rendered Z-stack of one WAT-chamber (i) (steps on the scale in 100 µm) and the corresponding maximum intensity projection with two sectional planes (ii), the individual adipocytes were unilocular and formed a densely packed 3D microtissue throughout the tissue chamber. **(b)** Comparison of lipid vacuole size of adipocytes on-chip versus explants (two replicates per condition). Scale bar equals 150 µm.

individual cell sizes are very similar between explant and on-chip culture. This indicates that the WAT-on-a-chip does indeed recapitulate the morphological heterogeneity of mature adipocytes in WAT *in vivo*.

Validation of adipocyte functionality on-chip. To assess the capability of the WAT-on-a-chip system to maintain viability and functionality of the integrated tissues, we deployed a comprehensive toolbox of chip-specific, functional readout methods. First, the viability and integrity of the vast majority of cells after eight days of on-chip culture was confirmed using a FDA/PI-based live/dead-staining protocol tailored specifically for the chip's configuration (Fig. 4a). In addition, to verify that the objective of any microphysiological OoC system – the recapitulation of *in vivo* functionality – was indeed attained, we examined multiple functional endpoints. Taking advantage of the optical accessibility and continuous medium perfusion through our system, we performed non-invasive imaging and analysis of media effluents under several conditions.

To monitor fatty acid metabolism in real-time, we added the fluorescently tagged fatty dodecanoic acid ($C_{12}H_{24}O_2$) analog (BODIPY™ 500/510 C1, C12) to the perfusion medium, and characterized the dynamics of fatty acid influx into, and efflux from, the WAT-model. This assay represents a powerful tool that allows non-invasive assessment of the cellular uptake of fatty acids, their accumulation in intracellular lipid vacuoles, and their release from adipocytes when the fatty-acid analog is removed from the medium. Utilizing time-resolved fluorescence microscopy, we were able to observe these characteristic uptake and secretion kinetics in the adipocytes cultured on-chip (Fig. 4b).

The continuous, convective transport by the perfusion flow of metabolized and secreted factors away from the tissues, provides opportunities for effluent sampling in a time-resolved manner, allowing the dynamics of e.g. metabolism, secretion, and endocrine functionality to be measured. Using colorimetric assays, we characterized the levels of oleic acid, a representative of non-esterified fatty acids (NEFAs), and of glycerol in the effluent medium, and found that their concentrations remained very stable for several days of culturing (Fig. 4c). The measured NEFA and glycerol levels were comparable to levels from human subcutaneous adipose tissue explants immediately after biopsy⁴⁶. In a similar approach, we examined the impact on fatty acid release of a 0.2 (w/v)% supplementation of the perfusion medium with human serum albumin (HSA). After 24 h of perfusion, we observed a significant increase of NEFA levels in the effluent (Fig. 4d). Thus, in our system, effluent sampling provided a powerful, non-invasively obtained readout of secretome and metabolome dynamics with high temporal resolution (depending on the sensitivity of the employed assay). This constitutes an effective link for the cross-correlation with clinical data and biomarker development. The general applicability of effluent sampling, however, is restricted by the base material PDMS, which is utilized for the majority of microfluidic platforms and also for our WAT-on-a-chip. The major limitation of many polymers and especially PDMS is the absorption of small hydrophobic molecules, which is especially an issue in microfabricated devices due to the large surface-to-volume ratio⁴⁷. Hence, many hormones as well as adipokines can partition into the polymer leading to an uncontrolled reduction of their concentration in the effluent down to undetectable amounts. This is, for instance, the case for the important adipokine adiponectin (Supplement S5). To account for this, future generations of the WAT-chip are envisioned to employ alternative materials or surface coatings.

Long-term functionality of integrated white adipose tissue. One of the main challenges of conventional adipocyte *in vitro* culture is the long-term maintenance of functional stability. As discussed above, issues related to buoyancy, fragility and de-differentiation of adipocytes typically limit the duration of integrity of *in vitro* cultures to a couple of days at most^{46,48}. Our structural and functional characterization of the

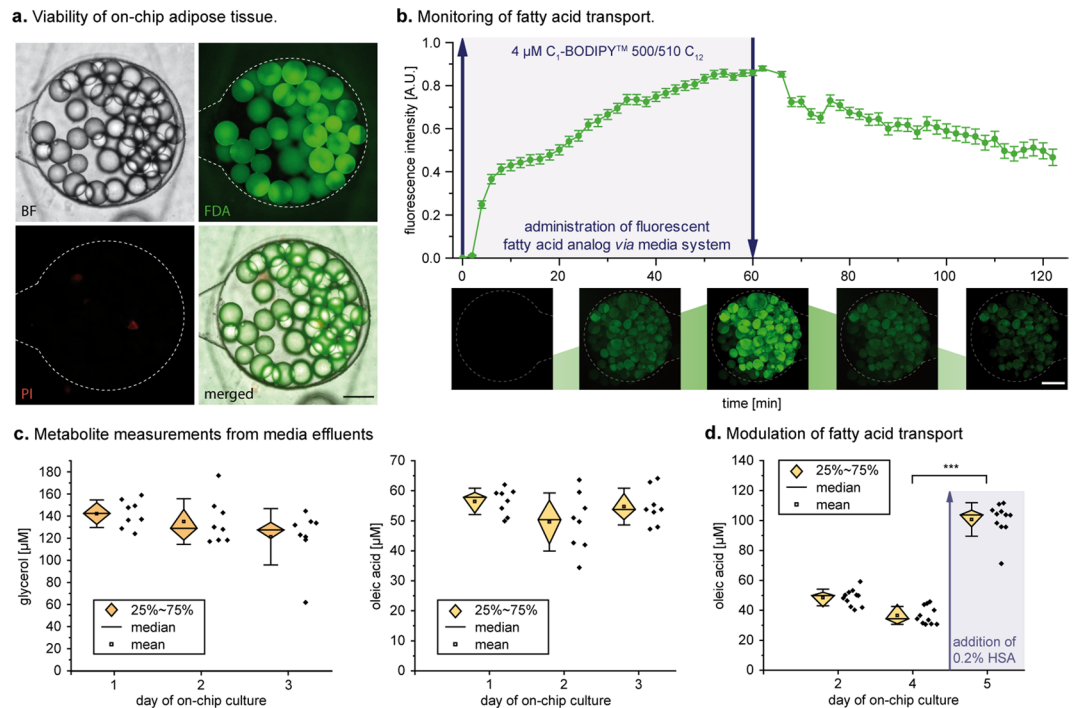


Figure 4. Functional validation of the human WAT-on-a-chip. **(a)** Live/dead-staining of adipocytes on day 8 of on-chip culture. FDA (green) marks live adipocytes by confirming membrane integrity and esterase activity in the vast majority of the integrated adipocytes. PI (red) staining indicates a very low number of apoptotic/necrotic and dead adipocytes. Scale bar equals 150 μm . **(b)** On-line monitoring of fatty acid transport on day 6. Monitoring of fatty acid uptake and accumulation was realized by the addition of a fluorescent fatty acid analog (4 μM BODIPYTM 500/510 C1, C12) to the perfused medium for one hour, followed by measurement of the mean fluorescence intensity. Upon removal of the fatty acid analog from the medium, fatty acid release could be observed ($n = 47$ individual tissue chambers). Scale bar equals 150 μm . **(c)** Evaluation of fatty acid metabolites in media effluents. Using colorimetric assays, glycerol and oleic acid (representative of non-esterified fatty acids) concentrations were found to be stable for the first three days of on-chip culture ($n = 8$ systems with 8 tissue chambers each). **(d)** Upon addition of 0.2% w/v human serum albumin (HSA) to the culture medium for 24 h, fatty acid release significantly increased compared to that during previous days ($p < 0.005$; $n = 11$ systems with eight tissue chambers each).

WAT-on-a-chip indicated that this microphysiological platform is capable of maintaining stable culture conditions over prolonged time periods. However, to investigate the potential of the platform to support a robust, long-term culture, we non-invasively monitored cell viability for a culture time of 36 days (Fig. 5a) by analyzing the release of lactate dehydrogenase (LDH) to the medium effluents. Throughout the culture, LDH levels were below 5% of LDH levels measured in the target cell maximum LDH release control (positive control) indicating a good overall on-chip viability. These findings were further supported by a live/dead-staining performed as an endpoint analysis of the long-term culture. To additionally investigate the long-term functionality, we performed fatty acid uptake assays on the tissues after 6 days, as well as after 36 days of on-chip culture (Fig. 5b). We observed that even after more than a month of *in vitro* culture, adipocytes still showed functional uptake and accumulation of fatty acids. Interestingly, a difference in initial uptake rates emerged, which might be related to size limitation of the “long-term-fed” cells on day 36. Still, these findings highlight that the WAT-on-a-chip is indeed capable of maintaining the functionality of adipose tissue for much longer periods than are conventional methods. This brings within reach a variety of novel opportunities for *in vitro* studies, e.g. of long-term effects of nutrition, repeated exposure of potential toxicants, or of long-term endocrine dynamics⁴⁹.

Applicability of WAT-on-a-chip for drug testing. Since an important area of application for the organ-on-a-chip technology is drug development, we conducted a proof of concept compound test to assess the applicability of our WAT-on-a-chip for pharmaceutical research. After 6 days of on-chip culture, we exposed the WAT-chip to the β -adrenergic agonist isoproterenol, which is known to induce lipolysis. By additionally supplementing the medium with the fluorescently tagged fatty acid analog (BODIPYTM 500/510 C1, C12) for 60 minutes, we were able to monitor isoproterenol-related effects on fatty acid uptake and release by adipocytes, using standard fluorescence microscopy (Fig. 6). While media with fluorescently tagged fatty acids was perfused, the normalized fluorescent intensity in the isoproterenol-treated systems increased significantly more slowly than in non-treated control systems. After switching to media without the fluorescently tagged fatty acid analog, the fluorescent intensity decreased much quicker in the isoproterenol-treated systems. Taken together, this means that the isoproterenol exposure induced a reduction of the net uptake rate of fatty acids and an increase of their release rate. Both findings are in line with the expected lipolysis-inducing effect of isoproterenol.

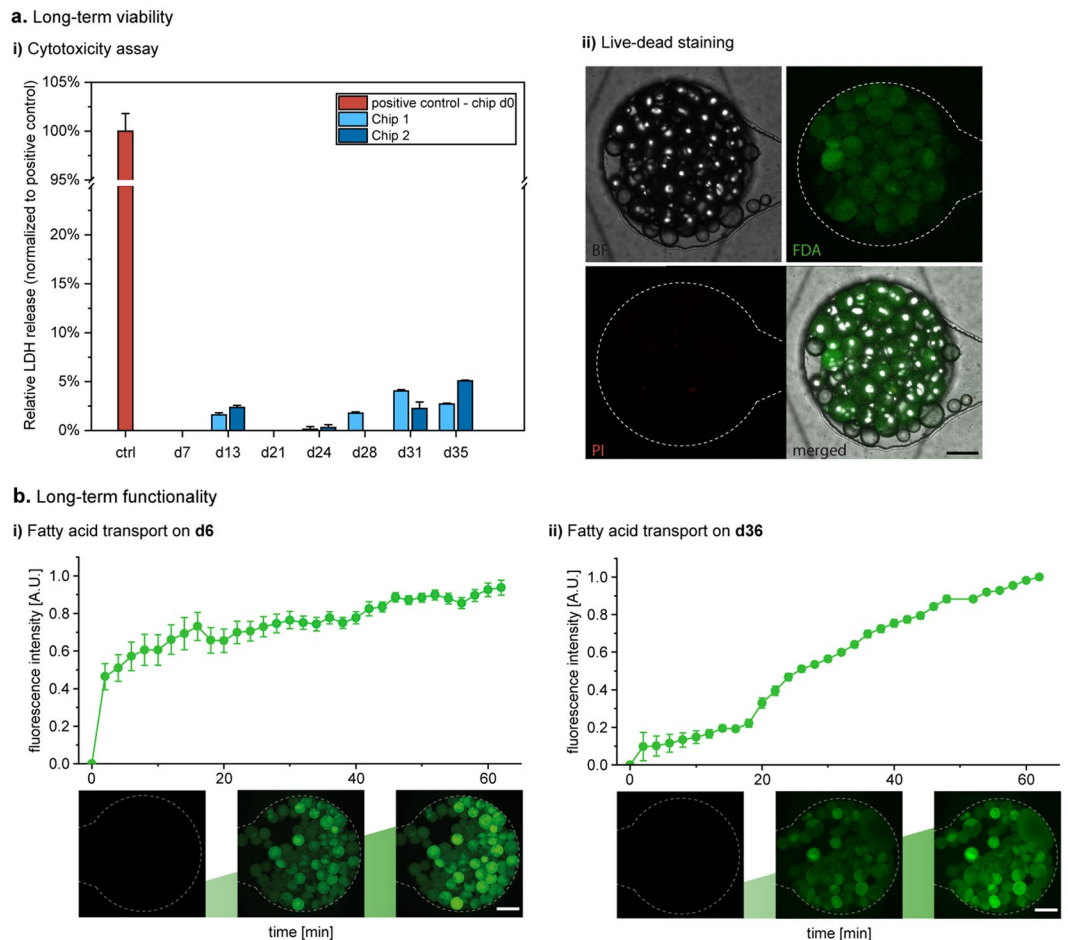


Figure 5. Long-term viability and functionality of the human WAT-on-a-chip. **(a)** Long-term viability determined via **(a.i)** non-invasive measurement of LDH release from medium effluents (absence of bars indicates no detectable difference to 0) as well as **(a.ii)** live/dead staining at day 36. Scale bar equals 150 μm . **(b)** Dynamic measurement of the normalized fluorescence intensity in tissue chambers perfused with medium containing a fluorescent fatty acid analog ($4\ \mu\text{M}$ BODIPYTM 500/510 C1, C12) revealed functional fatty acid uptake and accumulation in the WAT-model after **(b.i)** 6 as well as **(b.ii)** 36 days of on-chip culture ($n = 6$ individual tissue chambers). Scale bars equal 150 μm .

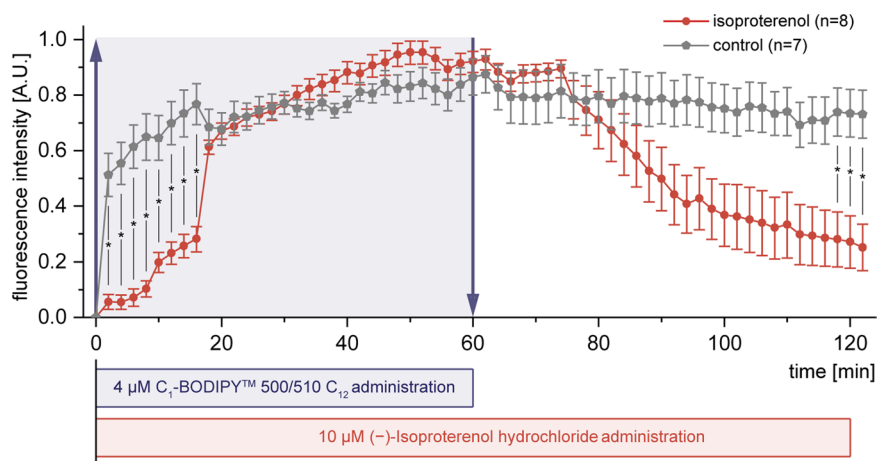


Figure 6. Applicability for drug testing illustrated by the effect of isoproterenol on fatty acid uptake and release. Normalized mean fluorescence intensity obtained by time-lapse fluorescence microscopy of WAT-on-a-chip systems perfused with medium supplemented with the fluorescently tagged fatty acid analog ($4\ \mu\text{M}$ BODIPYTM 500/510 C1, C12) during the first 60 minutes. Kinetics in systems exposed to $10\ \mu\text{M}$ Isoproterenol (red circles) show significant differences to non-treated controls (grey polygons) ($n = 7$ and $n = 8$ individual tissue chambers; mean fluorescence intensities \pm SEM are presented).

Evidently, the used approach based on standard microscopy provides facile and non-invasive read-outs for drug screening, with a very high time-resolution, which is amenable for massive parallelization and automation. One noteworthy limitation is the requirement for normalization of readings from individual tissue chambers. Absolute quantitative values would provide even more information and potential for cross-correlation; it is, therefore, planned to address this in future generations of chips and readout-infrastructure. Overall, the successful proof of concept highlights the applicability of the WAT-on-a-chip system for screening purposes and the potential the system can have for drug development purposes.

Conclusion

Due to the lack of suitable experimental human model systems, research in adipose tissue biology and obesity has so far relied mostly on animal models, non-physiological *in vitro* systems, GWAS studies and (clinical) epidemiology. The first two approaches have major limitations in terms of their translatability to humans; the latter two require complex statistical analyses of large data sets and do not permit strong conclusions on pathophysiological mechanisms or efficacy of therapeutic interventions in individuals. The human WAT-on-a-chip platform presented here provides a novel tool that enables the maintenance, monitoring and manipulation of human adipocytes in a durably stable, tissue-like microphysiological environment. As an engineered model system, there are naturally still differences compared to complex *in vivo* tissue, which could be further reduced in the future, e.g. by the integration of WAT-resident immune cells and further cells from the stromal vascular fraction. Nevertheless, the vasculature-like perfusion provides opportunities for biomarker evaluation and “liquid biopsies” that can be cross-correlated with clinical endpoints, as well as a potential connection link for integration with other organ-on-a-chip platforms³⁴. Multi-organ-chips integrating WAT-models are likely to be of major interest e.g. for ADMET, diabetes or non-alcoholic steatohepatitis (NASH) studies.

Overall, the introduced WAT-on-a-chip system offers new perspectives and opportunities in mechanistic studies, pharmaceutical development and testing, as well as in personalized medicine.

Received: 17 May 2019; Accepted: 31 March 2020;

Published online: 20 April 2020

References

- World Health Organization (WHO), *Obesity*, <https://www.who.int/news-room/facts-in-pictures/detail/6-facts-on-obesity> (accessed 16 February 2019).
- World Health Organization (WHO), *Global Health Observatory (GHO) data*, <https://www.who.int/gho/en/> (accessed 16 February 2019).
- World Health Organization (WHO), *Facts and figures on childhood obesity*, <https://www.who.int/end-childhood-obesity/facts/en/> (accessed 16 February 2019).
- Wang, Y., Beydoun, M. A., Liang, L., Caballero, B. & Kumanyika, S. K. Will All Americans Become Overweight or Obese? Estimating the Progression and Cost of the US Obesity Epidemic. *Obesity* **16**, 2323–2330 (2008).
- Young, B., O'Dowd, G. & Woodford, P. *Wheater's Functional Histology*, Churchill Livingstone, 6th Edition, ISBN 978070204743 (2014).
- Rosen, E. D. & Spiegelman, B. M. What We Talk About When We Talk About Fat. *Cell* **156**, 20–44 (2014).
- Kershaw, E. E. & Flier, J. S. Adipose Tissue as an Endocrine Organ. *J. Clin. Endocrinol. Metab.* **89**, 2548–2556 (2004).
- Scherer, P. E. Adipose Tissue: From Lipid Storage Compartment to Endocrine Organ. *Diabetes* **55**, 1537–1545 (2006).
- Fasshauer, M. & Blüher, M. Adipokines in health and disease. *Trends Pharmacol. Sci.* **36**, 461–470 (2015).
- Bélangier, C., Luu-The, V., Dupont, P. & Tchernof, A. Adipose Tissue Intracrinology: Potential Importance of Local Androgen/Estrogen Metabolism in the Regulation of Adiposity. *Horm. Metab. Res.* **34**, 737–745 (2002).
- Mayes, J. S. & Watson, G. H. Direct effects of sex steroid hormones on adipose tissues and obesity. *Obes. Rev.* **5**, 197–216 (2004).
- Marra, F. & Bertolani, C. Adipokines in liver diseases. *Hepatology* **50**, 957–969 (2009).
- Berg, A. H. & Scherer, P. E. Adipose tissue, inflammation, and cardiovascular disease. *Circ. Res.* **96**, 939–949 (2005).
- Zhang, Z. & Scherer, P. E. Adipose tissue: The dysfunctional adipocyte — a cancer cell's best friend. *Nat. Rev. Endocrinol.* **14**, 132–134 (2018).
- Hajer, G. R., van Haefen, T. W. & Visseren, F. L. J. Adipose tissue dysfunction in obesity, diabetes, and vascular diseases. *Eur. Heart J.* **29**, 2959–2971 (2008).
- Pérez-Hernández, A. I., Catalán, V., Gómez-Ambrosi, J., Rodríguez, A. & Frühbeck, G. Mechanisms linking excess adiposity and carcinogenesis promotion. *Front. Endocrinol. (Lausanne)* **5**, 65 (2014).
- Nawrocki, A. R. & Scherer, P. E. Keynote review: the adipocyte as a drug discovery target. *Drug Discov. Today* **10**, 1219–1230 (2005).
- Kusminski, C. M., Bickel, P. E. & Scherer, P. E. Targeting adipose tissue in the treatment of obesity-associated diabetes. *Nat. Rev. Drug Discov.* **15**, 639 (2016).
- Haas, B., Schlinkert, P., Mayer, P. & Eckstein, N. Targeting adipose tissue. *Diabetol. Metab. Syndr.* **4**, 43 (2012).
- Sankaralingam, S., Kim, R. B. & Padwal, R. S. The Impact of Obesity on the Pharmacology of Medications Used for Cardiovascular Risk Factor Control. *Can. J. Cardiol.* **31**, 167–176 (2015).
- Sheng, X. *et al.* Adipocytes Sequester and Metabolize the Chemotherapeutic Daunorubicin. *Mol. Cancer Res.* **15**, 1704–1713 (2017).
- Kleinert, M. *et al.* Animal models of obesity and diabetes mellitus. *Nat. Rev. Endocrinol.* **14**, 140 (2018).
- King, A. & Bowe, J. Animal models for diabetes: Understanding the pathogenesis and finding new treatments. *Biochem. Pharmacol.* **99**, 1–10 (2016).
- Poulos, S. P., Dodson, M. V. & Hausman, G. J. Cell line models for differentiation: preadipocytes and adipocytes. *Exp. Biol. Med.* **235**, 1185–1193 (2010).
- Li, X. & Easley, C. J. Microfluidic systems for studying dynamic function of adipocytes and adipose tissue. *Anal. Bioanal. Chem.* **410**, 791–800 (2018).
- Mandrup, S., Loftus, T. M., MacDougald, O. A., Kuhajda, F. P. & Lane, M. D. Obese gene expression at *in vivo* levels by fat pads derived from sc implanted 3T3-F442A preadipocytes. *Proc. Natl. Acad. Sci. U.S.A.* **94**, 4300–5 (1997).
- Volz, A.-C., Omengo, B., Gehrke, S. & Kluger, P. J. Comparing the use of differentiated adipose-derived stem cells and mature adipocytes to model adipose tissue *in vitro*. *Differentiation* **110**, 19–28 (2019).
- Abbott, R. D. *et al.* Variability in responses observed in human white adipose tissue models. *J. Tissue Eng. Regen. Med.* **12**, 840–847 (2017).
- Rogal, J., Zbinden, A., Schenke-Layland, K. & Loskill, P. Stem-cell based organ-on-a-chip models for diabetes research. *Adv. Drug Deliv. Rev.* **140**, 101–128 (2019).

30. Esch, E. W., Bahinski, A. & Huh, D. Organs-on-chips at the frontiers of drug discovery. *Nat. Rev. Drug Discov.* **14**, 248–260 (2015).
31. Ahadian, S. *et al.* Organ-On-A-Chip Platforms: A Convergence of Advanced Materials. *Cells, and Microscale Technologies. Adv. Healthc. Mater.* **7**, 1700506 (2018).
32. Berg, A. V. D., Mummery, C. L., Passier, R. & Van Der Meer, A. D. Personalised organs-on-chips: functional testing for precision medicine. *Lab Chip* **19**, 198–205 (2019).
33. Esch, M. B. *et al.* Multi-Organ toxicity demonstration in a functional human *in vitro* system composed of four organs. *Adv. Drug Deliv. Rev.* **69–70**, 158–169 (2014).
34. Rogal, J., Probst, C. & Loskill, P. Integration concepts for multi-organ chips: how to maintain flexibility?! *Futur. Sci. OA FSO180* (2017).
35. Dugan, C. E. & Kennedy, R. T. *Measurement of lipolysis products secreted by 3T3-L1 adipocytes using microfluidics*, Elsevier Inc., 1st edn., vol. 538(2014).
36. Loskill, P. *et al.* WAT-on-a-chip: a physiologically relevant microfluidic system incorporating white adipose tissue. *Lab Chip* **17**, 1645–1654 (2017).
37. Abbott, R. D. *et al.* Long term perfusion system supporting adipogenesis. *Methods* **84**, 84–89 (2015).
38. Liu, Y. *et al.* Adipose-on-a-chip: a dynamic microphysiological *in vitro* model of the human adipose for immune-metabolic analysis in type II diabetes. *Lab Chip* **19**, 241–253 (2019).
39. Kongsuphol, P. *et al.* *In vitro* micro-physiological model of the inflamed human adipose tissue for immune-metabolic analysis in type II diabetes. *Sci. Rep.* **9**, 4887 (2019).
40. Godwin, L. A. *et al.* A microfluidic interface for the culture and sampling of adiponectin from primary adipocytes. *Analyst* **140**, 1019–1025 (2015).
41. Harms, M. J. *et al.* Mature Human White Adipocytes Cultured under Membranes Maintain Identity, Function, and Can Transdifferentiate into Brown-like Adipocytes. *Cell Rep.* **27**, 213–225.e5 (2019).
42. Zhang, H. H., Kumar, S., Barnett, A. H. & Eggo, M. C. Surface Proteins of Gram-Positive Bacteria and How They Get There. *J. Endocrinol.* **164**, 119–128 (2000).
43. Huber, B. *et al.* Integration of Mature Adipocytes to Build-Up a Functional Three-Layered Full-Skin Equivalent. *Tissue Eng. Part C Methods* **22**, 756–764 (2016).
44. Sugihara, H., Yonemitsu, N., Miyabara, S. & Yun, K. Primary cultures of unilocular fat cells: characteristics of growth *in vitro* and changes in differentiation properties. *Differentiation* **31**, 42–49 (1986).
45. Matsumoto, T. *et al.* Mature adipocyte-derived dedifferentiated fat cells exhibit multilineage potential. *J. Cell. Physiol.* **215**, 210–222 (2008).
46. Decaunes, P., Bouloumié, A., Ryden, M. & Galitzky, J. *Ex vivo* Analysis of Lipolysis in Human Subcutaneous Adipose Tissue Explants. *Bio-protocol* **8**, 1–12 (2018).
47. Toepke, M. W. & Beebe, D. J. PDMS absorption of small molecules and consequences in microfluidic applications. *Lab Chip* **6**, 1484–1486 (2006).
48. Maurizi, G. *et al.* Human white adipocytes convert into “rainbow” adipocytes *in vitro*. *J. Cell. Physiol.* **232**, 2887–2899 (2017).
49. Nawroth, J., Rogal, J., Weiss, M., Brucker, S. Y. & Loskill, P. Organ-on-a-Chip Systems for Women's Health Applications. *Adv. Healthc. Mater.* **1700550** (2017).

Acknowledgements

The authors thank Dr. Ziegler (Klinik Charlottenhaus, Stuttgart) for the kind provision of human adipose tissue from plastic surgery, Dr. Jakob Barz for help with the PECVD coating process, and Silvia Kolbus-Hernandez, Elena Rubiu as well as Luisa Merz for their assistance with cell culture and chip fabrication. We further thank Prof. Andreas Stahl and Pete Zushin for helpful discussions and Joost Overduin for language-editing. The research was supported in part by the Fraunhofer-Gesellschaft internal programs Talenta Start (to J.R.) and Attract (601543), the DAAD funded by the Bundesministeriums für Bildung und Forschung (BMBF) (PPP USA 2018, 57387214) (all to P.L.), as well as the Ministry of Science, Research and the Arts of Baden-Württemberg (Az: 7542.2-501-1/13/6 to P.L. and Az: 33-729.55-3/214-8 to K.S.-L.).

Author contributions

J.R. and P.L. designed the device. J.R. and C.B. fabricated the device. J.R., C.B., E.K. and J.Rz. performed and analyzed the experiments. S.S. performed membrane characterization. C.P. performed simulations. K.S.-L. gave biological advice. J.R., K.S.-L. and P.L. wrote the manuscript. J.R. and P.L. designed the study.

Competing interests

The authors declare no competing interests.

Additional information

Supplementary information is available for this paper at <https://doi.org/10.1038/s41598-020-63710-4>.

Correspondence and requests for materials should be addressed to P.L.

Reprints and permissions information is available at www.nature.com/reprints.

Publisher's note Springer Nature remains neutral with regard to jurisdictional claims in published maps and institutional affiliations.



Open Access This article is licensed under a Creative Commons Attribution 4.0 International License, which permits use, sharing, adaptation, distribution and reproduction in any medium or format, as long as you give appropriate credit to the original author(s) and the source, provide a link to the Creative Commons license, and indicate if changes were made. The images or other third party material in this article are included in the article's Creative Commons license, unless indicated otherwise in a credit line to the material. If material is not included in the article's Creative Commons license and your intended use is not permitted by statutory regulation or exceeds the permitted use, you will need to obtain permission directly from the copyright holder. To view a copy of this license, visit <http://creativecommons.org/licenses/by/4.0/>.

© The Author(s) 2020